Babylonian Journal of Mechanical Engineering
Vol.2024, **pp**. 81–90
DOI: https://doi.org/10.58496/BJME/2024/010; ISSN: 3006-5410
https://mesopotamian.press/journals/index.php/BJME

Research Article

Effect of Inlet Velocity on The Entrance Length of Laminar and Turbulent Flow in A Circular Pipe

Farqad T. Najim[1,*]

[1] *Electrical Engineering Department, College of Engineering, Al-Iraqia University, Baghdad, Iraq,*

ARTICLE INFO

Article History
Received 17 Jul 2024
Revised: 17 Aug 2024
Accepted 18 Sep 2024
Published 21 Oct 2024

Keywords
Entrance length
Inlet velocity
Pressure drop

ABSTRACT

This study uses numerical simulations performed with ANSYS-FLUENT to investigate the hydrodynamic entrance length for fluid flow in a circular pipe under both laminar and turbulent conditions. The effect of inlet velocity on entrance length and pressure drop was analysed. Two physical models with diameters of 15 cm and lengths of 10 m and 13 m were employed. The numerical results were validated against theoretical predictions, showing good agreement. The results indicate that entrance length increases with inlet velocity due to the extended development of the boundary layer. For laminar flow, entrance lengths of 1.46 m, 3.85 m, and 12.54 m were observed for velocities of 1, 3, and 10 m/s, respectively, while a turbulent flow velocity of 16.6 m/s yielded an entrance length of 5.8 m. Additionally, it was found that higher inlet velocities significantly amplify pressure drop due to increased friction and energy losses.

1. INTRODUCTION

The entrance length of a pipe is a vital element in fluid mechanics, particularly in systems where accurate flow behaviour is crucial. It denotes the distance necessary for fluid entering a pipe to go from an initial non-uniform velocity profile to a fully established flow condition. Comprehending the factors that affect this transition, including fluid velocity, is essential for enhancing the design and functionality of pipe systems in engineering applications. Velocity significantly influences the entrance length since increased velocities often result in heightened turbulence, impacting the time and distance required for flow stabilization. The correlation between velocity and entrance length affects several sectors, such as chemical processing, water distribution, and oil transportation, where effective flow management may substantially influence performance and expenses. Multiple variables affect the entrance length, including fluid characteristics, pipe diameter, and, most importantly, flow velocity [1-6].

The hydrodynamic entrance length for laminar flows in circular and non-circular cross-sections depends on geometric factors, including diameter, aspect ratio, and hydraulic diameter [. Ferreira et al. (2021) numerically analysed laminar flow in microchannels with rectangular cross-sections. They established correlations for entrance length across various Reynolds numbers and aspect ratios, highlighting that lower Reynolds numbers disproportionately augment entrance length in microscale applications.

Jason and Chatterjee (2022) examined rectangular microchannels with plenums and emphasised that aspect ratios induce a non-monotonic fluctuation in entrance length. Abrupt contractions at the entrance create recirculation zones, modifying the dynamics of flow development. They suggested different metrics to delineate entrance lengths based on the evolution of cross-sectional velocity. Impact of Aspect Ratio. Non-circular geometries, including ellipses and triangular channels, display distinct flow development features resulting from variations in boundary layer interactions. Lambride et al. (2023) investigated power-law fluids in non-circular conduits, observing that the entrance length is affected by shear-thinning or shear-thickening characteristics and cross-sectional symmetry. Estimates of Entrance Length. Gong et al. (2020) assessed superhydrophobic surfaces and slip conditions in microchannels, finding that modifications to hydraulic diameter and slip length significantly reduce entrance lengths relative to conventional assumptions for smooth channels. Impacts of Slip Length and Hydraulic Diameter. Shajari et al. (2020) observed variations from steady-state predictions for entrance lengths

*Corresponding author. Email: it@gmail.com

under oscillatory flow conditions, highlighting the significance of oscillation frequency and amplitude in defining development zones for parallel plate microchannels. Entrance Length of Oscillatory Flows.
This research investigates the impact of velocity on entry length in pipes using both theoretical and experimental viewpoints. This work seeks to elucidate the link, allowing engineers to precisely forecast entrance length and improve the efficiency of fluid transport systems. The main objective of this work is to investigate the hydrodynamic entrance length for fluid flow inside a circular pipe using numerical simulation conducted by ANSYS-FLUENT commercial software. The effect of inlet velocity on the entrance length is investigated under laminar and turbulent conditions. Also, the effect of velocity on the pressure drop is tested.

2. ENTRANCE REGION

Consider a fluid entering a cylindrical conduit at a constant rate. Due to the no-slip condition, the fluid particles in the layer next to the pipe's surface cease all motion. This layer also induces a steady deceleration of the fluid particles in the neighbouring layers due to friction. To compensate for this decrease in velocity, the fluid's velocity at the pipe's midpoint must rise to maintain a constant mass flow rate down the pipe. Consequently, a velocity gradient forms along the pipe. The area of flow where the influence of viscous shearing forces due to fluid viscosity is experienced is referred to as the velocity boundary layer or simply the boundary layer. The hypothetical boundary surface separates the flow in a pipe into two distinct regions: the boundary layer region, characterised by significant viscous effects and velocity variations, and the irrotational (core) flow region, where frictional effects are minimal, and the velocity remains nearly constant in the radial direction [12].
The thickness of the boundary layer grows in the flow direction until it reaches the centre of the pipe, therefore occupying the whole pipe, as seen in Figure (1). The area extending from the pipe intake to the point where the boundary layer converges at the centerline is referred to as the hydrodynamic entrance region, and the extent of this area is termed the hydrodynamic entrance length L_h. The flow at the entrance zone is referred to as hydrodynamically evolving flow since this is where the velocity profile evolves. The area beyond the entrance zone where the velocity profile is entirely established and stays constant is referred to as the hydrodynamically fully formed region. The flow is considered completely formed when the normalised temperature profile stays constant. Hydrodynamically developed flow is synonymous with fully developed flow when the fluid within the pipe is neither heated nor cooled, as the fluid temperature in this scenario exhibits a parabolic profile in laminar flow and a comparatively flatter (or fuller) profile in turbulent flow due to eddy motion and enhanced radial mixing. The time-averaged velocity profile stays constant when the flow is completely formed, and hence, the condition of hydrodynamically fully developed flow is [13]:

$$\frac{\partial u(r,x)}{\partial x} = 0 \qquad (1)$$

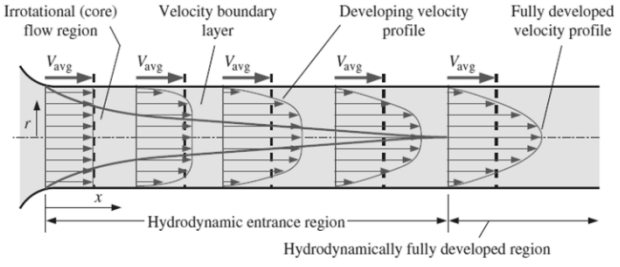

Fig. 1. The development of the velocity profile in a pipe [13].

3. ENTRANCE LENGTH

The hydrodynamic entrance length is defined as the distance from the pipe entrance to the point when the wall shear stress, and therefore the friction factor, attains a value within about 2 percent of the fully formed state. In laminar flow, the hydrodynamic entrance length is roughly defined [13]:

$$\frac{L_h laminar}{D} \cong 0.6 + 0.056\, Re_D \qquad (2)$$

The entrance length is much shorter in turbulent flow, as anticipated, and its dependency on the Reynolds number is less pronounced. In several pipe flows of practical engineering significance, the entrance effects become negligible at a pipe length of 40 diameters, and the hydrodynamic entrance length is [14]:

$$L_h turbulent \cong 40\ D \qquad (3)$$

Where Re_D is Reynolds number based on the diameter.

4. NUMERICAL SIMULATION

4.1 Physical Model

In contrast to experimental approaches, errors in the computational CFD methodology may arise throughout the process due to the creation of an erroneous model or the application of improper boundary conditions. The geometry and boundary conditions of models may greatly affect the results; hence, experimental data are collected and analysed to establish precise geometry and boundary conditions, ensuring satisfactory outcomes [15].

The two-dimensional model was designed and created by Ansys design modeler shown in Figure (2). Two models were created of 15 cm diameter, and 10 m, and 13 m length.

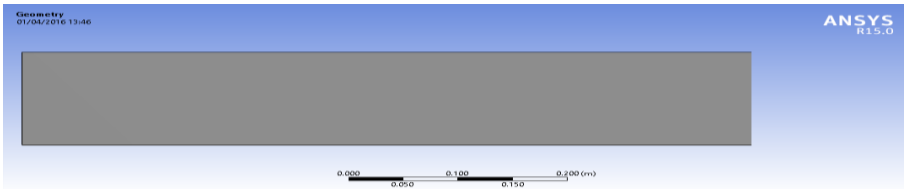

Fig. 2. Section of the Physical model

Mesh creation is important to the calculations performed by CFD software. The partial differential equations related to heat transport in fluids are consistently challenging to solve. In CFD software, the flow domain is partitioned into minuscule components, after which the governing equations are resolved for these discrete elements. A reduced element size in Ansys Fluent software yields superior and more accurate results. The iterative computation will need more time if a smaller element size is used. The element size used in this model was ($1.875x10^{-6}$)meters, achieved by configuring the number of components in two dimensions, which is regarded as a fine mesh size.
Upon specifying an element size and updating the model, the meshing will be executed as shown in figure (3). The meshing findings indicate that the parts inside the model are very dense, enabling precise outcomes.

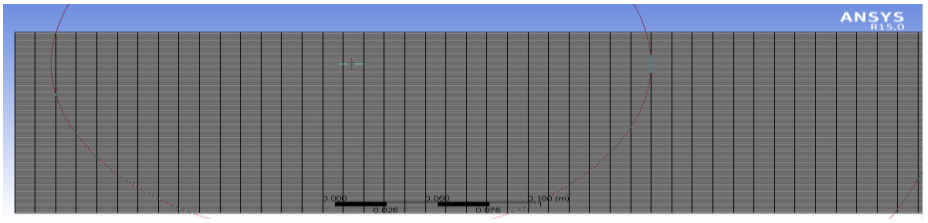

Fig. 3. The meshed model

The meshing tool available in ANSYS is used to generate a tetrahedral mesh throughout the computational domain. The grid independence investigations were carried out to obtain the optimum grid size using laminar model. The grid independence is carried out to check the change in flow distribution along the pipe with mesh cell number at Re=150.

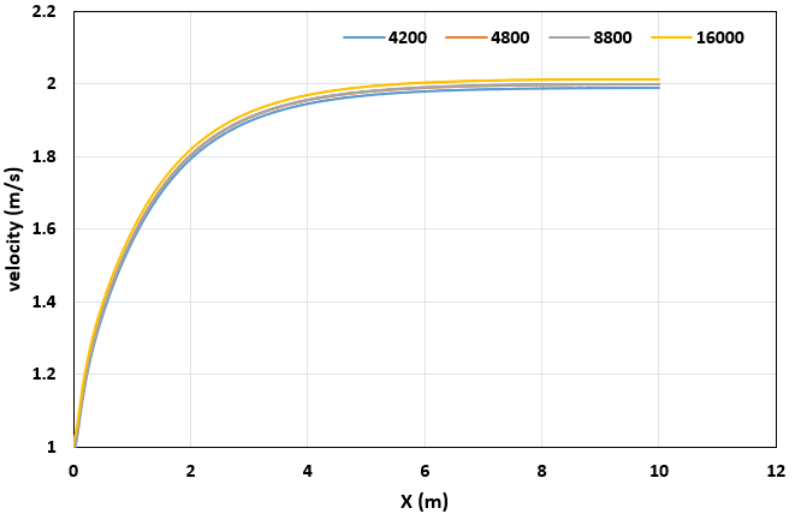

Fig. 4. Axial velocity distribution along the pipe for different elements number

4.2 Governing Equations

The Navier-Stokes equations, expressed in tensor notation, decompose variables into mean and fluctuation components through Reynolds averaging. This process resembles velocity decomposition [16]:

$$u_i = \bar{u}_i + u_i' \quad (3)$$

Where $\boldsymbol{u_i}$ is the instantaneous fluid velocity, $\boldsymbol{u_i'}$ is the velocity fluctuation and $\boldsymbol{\bar{u}_i}$ is the time-averaged value of $\boldsymbol{u_i}$ at a point. The governing equations include continuity, momentum and energy.

Continuity Equation

$$\frac{\partial \rho u}{\partial x} + \frac{\partial \rho v}{\partial x} + \frac{\partial \rho w}{\partial x} = 0 \quad (5)$$

The above equation may be expressed as follows, given that the mass density of fluid remains constant:

$$\frac{\partial u}{\partial x} + \frac{\partial v}{\partial x} + \frac{\partial w}{\partial x} = 0 \quad (6)$$

Then, the continuity equation is stated as:

$$\frac{\partial u_i}{\partial x_i} = 0 \quad (7)$$

Momentum Equation

$$\rho \frac{\partial u_i u_j}{x_j} = -\frac{\partial P}{\partial x_i} + \mu \frac{\partial}{\partial x_j}\left(\frac{\partial u_i}{\partial x_j} + \frac{\partial u_j}{\partial x_i}\right) + \rho \frac{\partial}{\partial x_j}(-\overline{u_i' u_j'}) \quad (8)$$

4.3 Boundary Conditions

The Governing equations are solved by utilising the following boundary conditions as in Figure (4):

- Left edge: velocity inlet
- Top and bottom edge: wall
- Bottom: symmetry

Fig. 4. The boundary conditions

5. RESULTS

The effect of inlet velocity on the entrance length is investigated for laminar and turbulent conditions. Table (1) shows the investigated velocities with corresponding Reynolds number. Figure (5) shows the radial velocity distribution along a pipe of diameter D=15 cm and V=1 m/s. The velocity decreases radially from the centre to the walls. Because of the no-slip condition, the fluid particles in the layer in contact with the surface of the pipe come to a complete stop. This layer also causes the fluid particles in the adjacent layers to retard gradually as a result of friction due to the viscosity effect.

TABLE I. THE INVESTIGATED VELOCITIES

Velocity (m/s)	Reynolds number Re
1	150
3	450
10	1500
16.6	2500

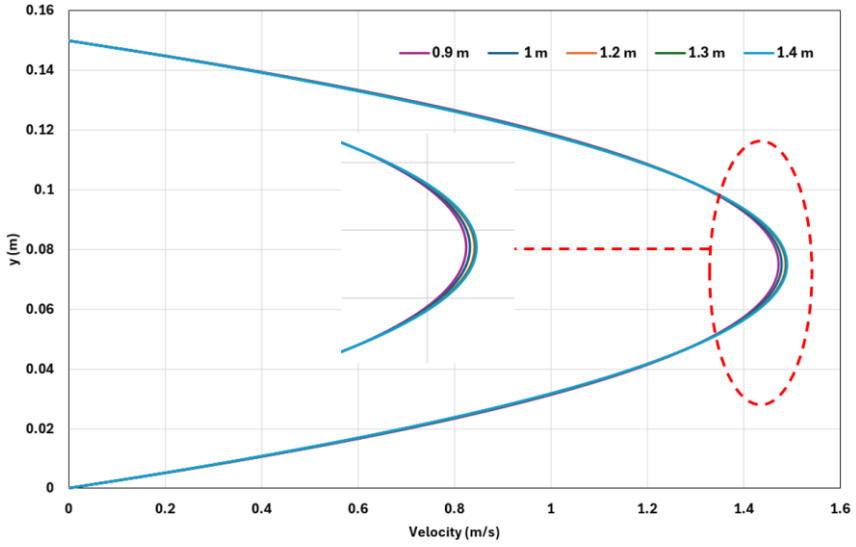

Fig. 5. Radial distribution of velocity for

Figures (6), (7), and (8) show the velocity axial distribution along the pipe of D=30 cm for laminar conditions, including velocity values 1, 3, and 10 m/s. The velocity changes along the pipe due to the effect of viscous shear forces. It is obvious from the figures the velocity doesn't change after the length of 1.46 m, 3.85 m, and 12.54 m, respectively, which represents the entrance length. The entrance length is increased with the inlet velocity. So the higher the inlet velocity, the longer the entrance length for the flow to fully developed. This can attributed to the viscous effect of the boundary layer, which takes a longer time to develop.

Figure (9) shows the axial profile for the turbulent flow of velocity 16.6 m/s. The velocity becomes constant after the length of 5.8 m, which is the entrance length. The values of entrance length obtained from the numerical simulations are in good agreement with those calculated from eq (2) and (3), as presented in Table (2).

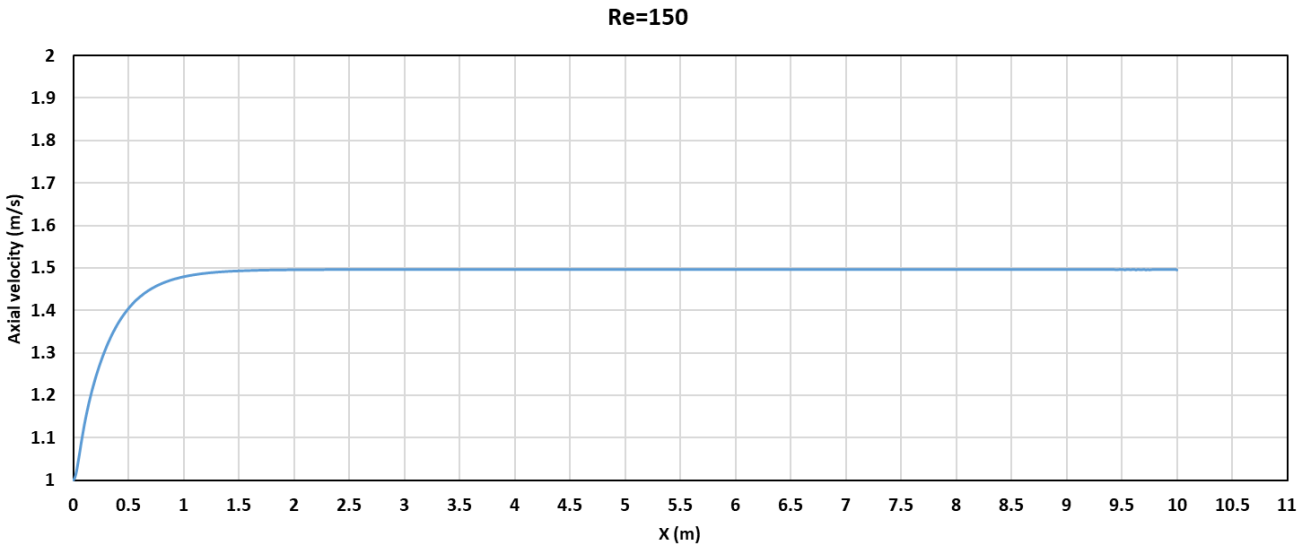

Fig. 6. Axial distribution of velocity v = 1 m/s

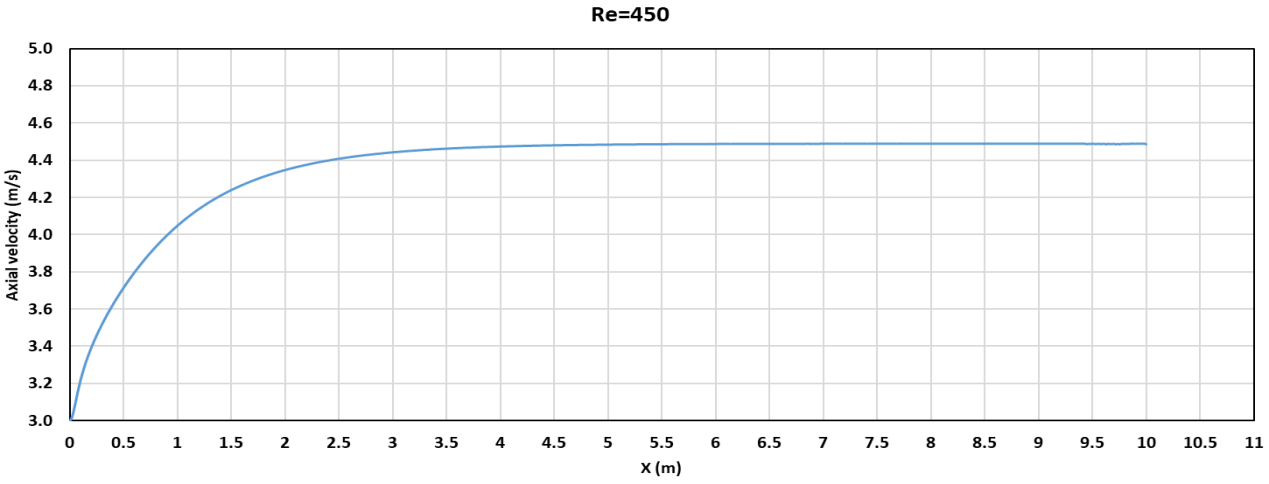

Fig. 7. Axial distribution of velocity v = 3 m/s

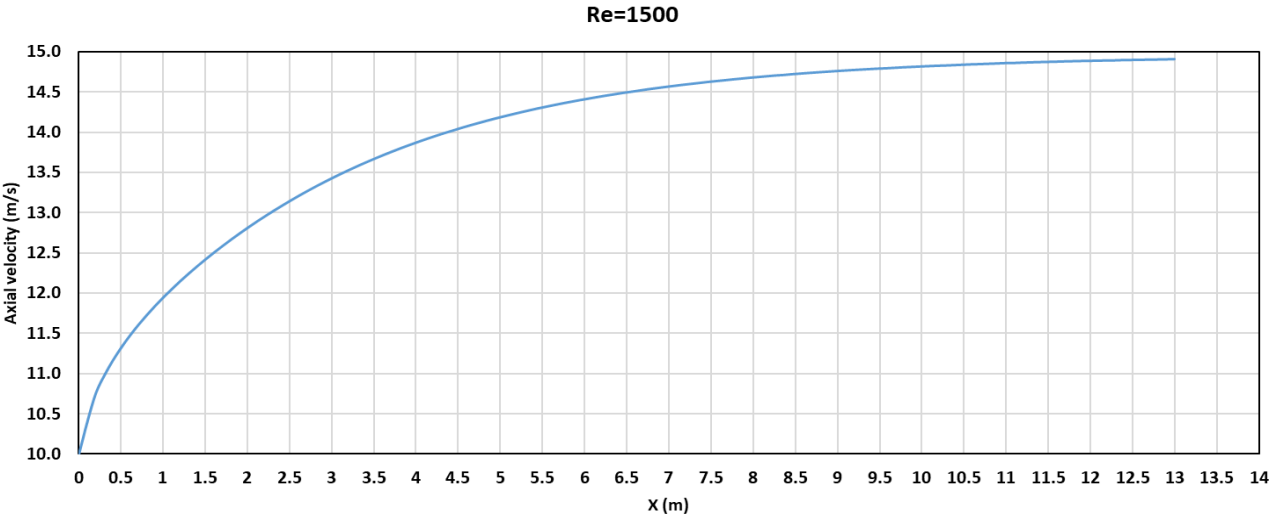

Fig. 8. Axial distribution of velocity v = 10 m/s

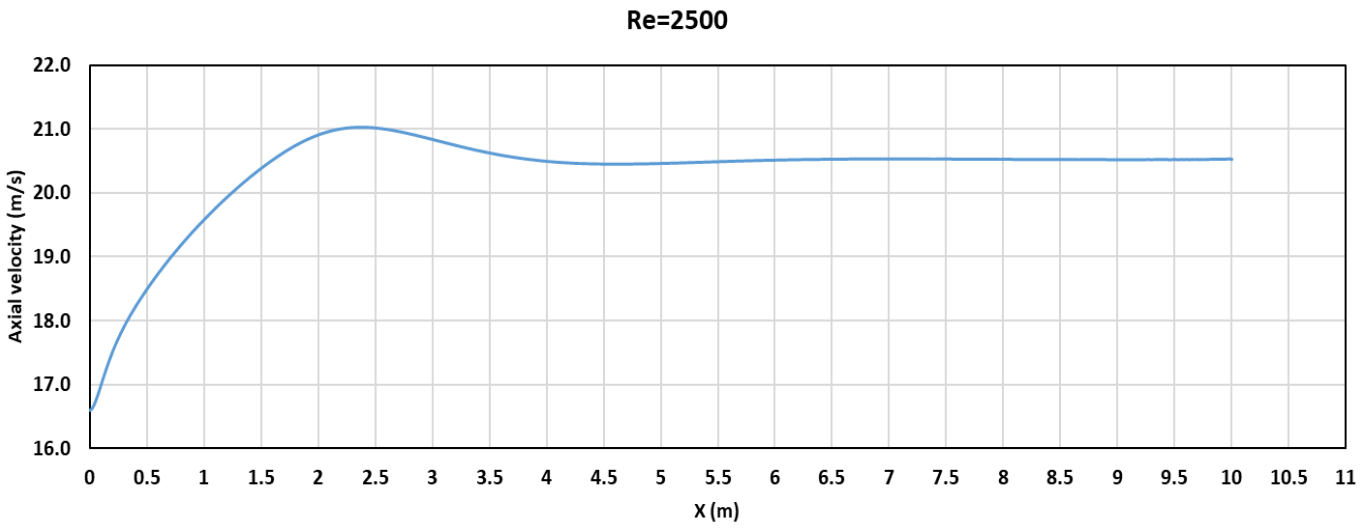

Fig. 9. Axial distribution of velocity v = 16.6 m/s

TABLE II. NUMERICAL AND CALCULATED ENTRANCE LENGTH

Re	Numerical	calculated
150	1.46	1.35
350	3.85	3.87
1500	12.54	12.69
2500	5.9	6

Figure (10) shows the contours of the radial profile of velocity at different locations. These contours are for Re= 150. It can be concluded that the fully developed flow occurs between X=12 m and X=13 m, which is consistent with the result obtained from equation (1-2), which refers to the fully developed flow occurring at X=12.69 m.

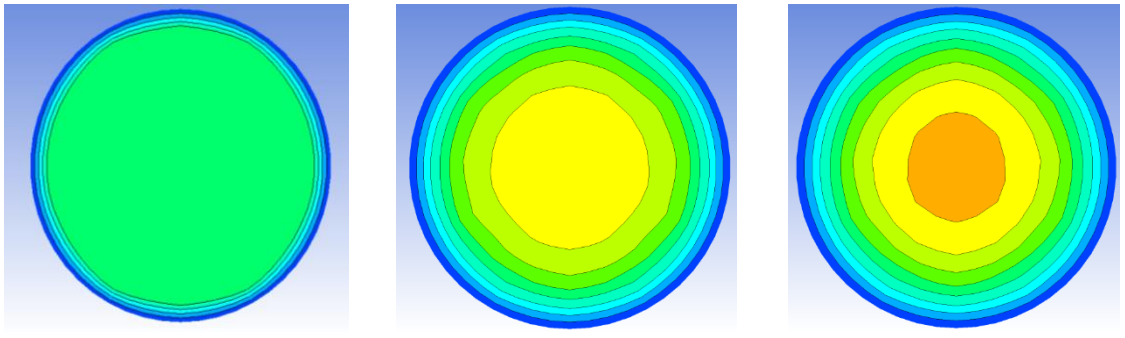

Inlet X=2 m X=4 m

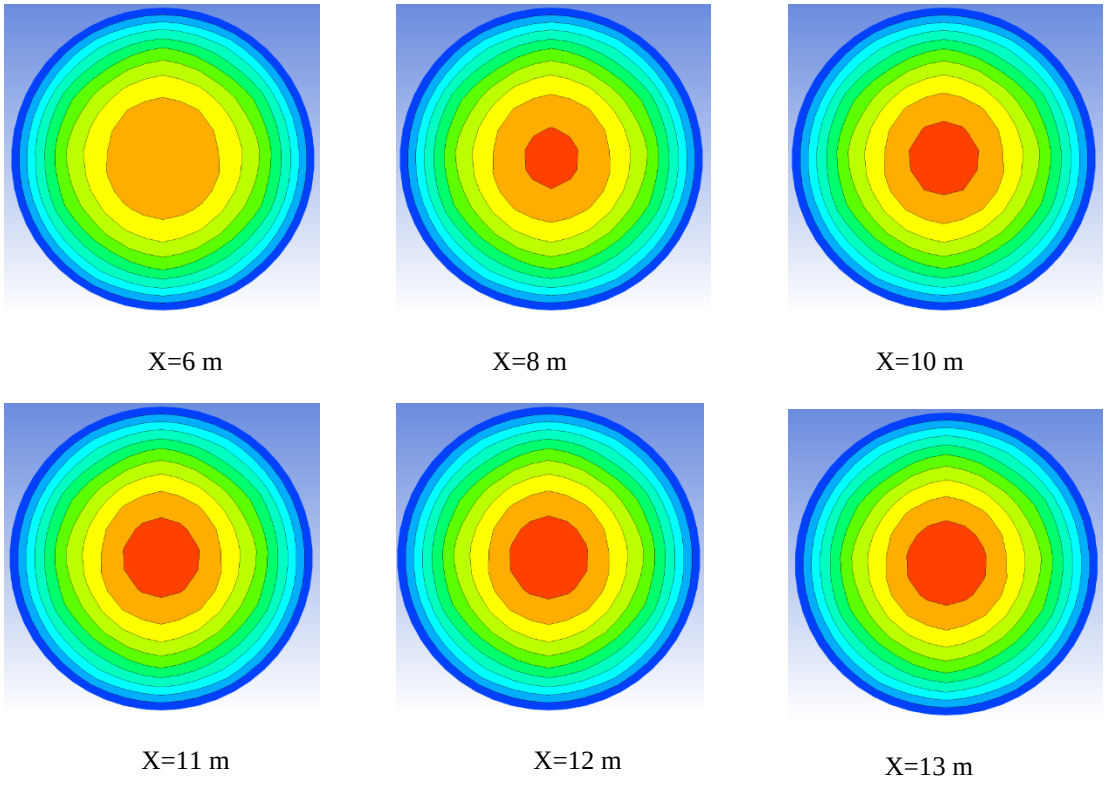

Fig. 10. Contours of the flow developing.

The effect of velocity on pressure drop is depicted in Figure (11) for different Reynolds numbers. The pressure drops increase at higher velocities. As fluid velocity increases, the pressure drop increases owing to higher friction between the fluid and the pipe walls and increased energy losses from internal viscous forces. Rapidly moving fluid particles collide with one another and the pipe surface with greater frequency and intensity, resulting in increased energy dissipation and turbulent motion. This energy loss necessitates a decrease in pressure energy, resulting in an increased pressure drop. Moreover, turbulence exacerbates resistance, so accelerating the rate of pressure decline.

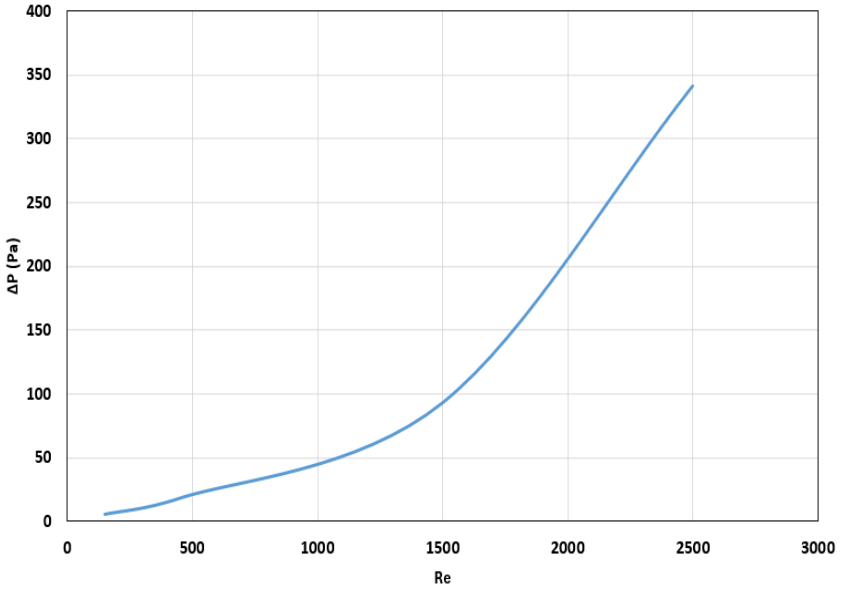

Fig. 11. The effect of velocity on pressure drop is depicted

6. CONCLUSIONS

In the present work, the entrance length for laminar and turbulent flow in a circular pipe is investigated numerically using ANSYS-FLUENT. The effect on inlet velocity is tested for the values 1, 3,10 and 16.6 m/s. The main conclusions can be summarised as follows:

- A good Agreement between the numerical results and the theoretical results is obtained.
- The inlet velocity has a significant effect on the entrance length.
- The pressure drop increases with the inlet velocity.

Conflicts Of Interest

The author's paper explicitly states that there are no conflicts of interest to be disclosed.

Funding

The author's paper clearly indicates that the research was conducted without any funding from external sources.

Acknowledgment

The author acknowledges the institution for their commitment to fostering a research-oriented culture and providing a platform for knowledge dissemination.

References

[1] J. G. Afshin and T. Lap-Mou, "Flow regime map for a horizontal pipe with uniform wall heat flux and three inlet configurations," Experimental Thermal and Fluid Science, vol. 10, no. 3, pp. 287–297, 1995.
[2] J. R. Augustine, Pressure Drop Measurements in the Transition Region for a Circular Tube with a Square-Edged Entrance, Ph.D. dissertation, Univ. Southwestern Louisiana, Lafayette, Louisiana, 1988.
[3] R. Barbin and J. B. Jones, "Turbulent flow in the inlet region of a smooth pipe," Journal of Basic Engineering, vol. 85, no. 1, pp. 29–33, 1963.
[4] M. J. Al-Dulaimi and K. E. Amori, “Effect of receiver geometry on the optical and thermal performance of a parabolic trough collector,” Heat Transfer, vol. 51, no. 3, pp. 2437–2457, Jan. 2022, doi: 10.1002/htj.22406.
[5] T. Hou Kuan, T. Lap Mao, and J. G. Afşin, "Effect of inlet geometries and heating on the entrance and fully-developed friction factors in the laminar and transition regions of a horizontal tube," Experimental Thermal and Fluid Science, vol. 44, pp. 680–696, 2013.
[6] L. M. Huang and T. S. Chen, "Stability of developing pipe flow subjected to non-axisymmetric disturbances," Journal of Fluid Mechanics, vol. 63, pp. 183–200, 1974.
[7] G. Ferreira, A. Sucena, L. L. Ferrás, F. T. Pinho, and A. M. Afonso, ‘Hydrodynamic entrance length for laminar flow in microchannels with rectangular cross-section’, Fluids, vol. 6, no. 7, p. 240, Jul. 2021.
[8] O. J. Lobo and D. Chatterjee, ‘Effect of aspect ratio on entrance length in rectangular minichannels with plenum’, Phys. Fluids (1994), vol. 34, no. 11, p. 112009, Nov. 2022.
[9] C. Lambride, A. Syrakos, and G. C. Georgiou, ‘Entrance length estimates for flows of power-law fluids in pipes and channels’, J. Nonnewton. Fluid Mech., vol. 317, no. 105056, p. 105056, Jul. 2023.
[10] W. Gong, J. Shen, W. Dai, Z. Deng, X. Dong, and M. Gong, ‘Effects of slip length and hydraulic diameter on hydraulic entrance length of microchannels with superhydrophobic surfaces’, Front. Energy, vol. 14, no. 1, pp. 127–138, Mar. 2020.
[11] G. Shajari, M. Abbasi, and M. K. Jamei, “Entrance length of oscillatory flows in parallel plate microchannels,” Proceedings of the Institution of Mechanical Engineers, Part C: Journal of Mechanical Engineering Science, vol. 235, no. 19. SAGE Publications, pp. 3833–3843, Oct. 26, 2020. doi: 10.1177/0954406220968125.
[12] R. W. Fox, A. T. McDonald, and P. J. Pritchard, Introduction to Fluid Mechanics, 9th ed. Hoboken, NJ, USA: Wiley, 2020.

[13] F. M. White, Fluid Mechanics, 7th ed. New York, NY, USA: McGraw-Hill Education, 2011.
[14] Nikuradse, J., Gesetzmäßigkeiten der turbulenten Strömung in glatten Rohren, Forschung auf dem Gebiet des Ingenieurwesens, 3, 1932, 1–36, (Translated in NASA TT F-10, 359,1966.
[15] M. Hajdukiewicz, F. J. González Gallero, P. Mannion, M. G. L. C. Loomans, and M. M. Keane, “A narrative review to credible computational fluid dynamics models of naturally ventilated built environments,” Renewable and Sustainable Energy Reviews, vol. 198. Elsevier BV, p. 114404, Jul. 2024. doi: 10.1016/j.rser.2024.114404.
[16] ANSYS Theory Guide, 2016.